Estimating Global GPP with SIF and a Data Assimilation System

Alexander J. Norton

P.J. Rayner, E.N. Koffi, M. Scholze, J.D. Silver, Y-P. Wang

THE UNIVERSITY OF MELBOURNE

CSIRO

ARC CENTRE OF EXCELLENCE FOR CLIMATE SYSTEM SCIENCE

Estimating Global GPP

- Global GPP estimates vary widely (see review by Anav et al. 2015)
- Observations need to be better integrated with predictive models

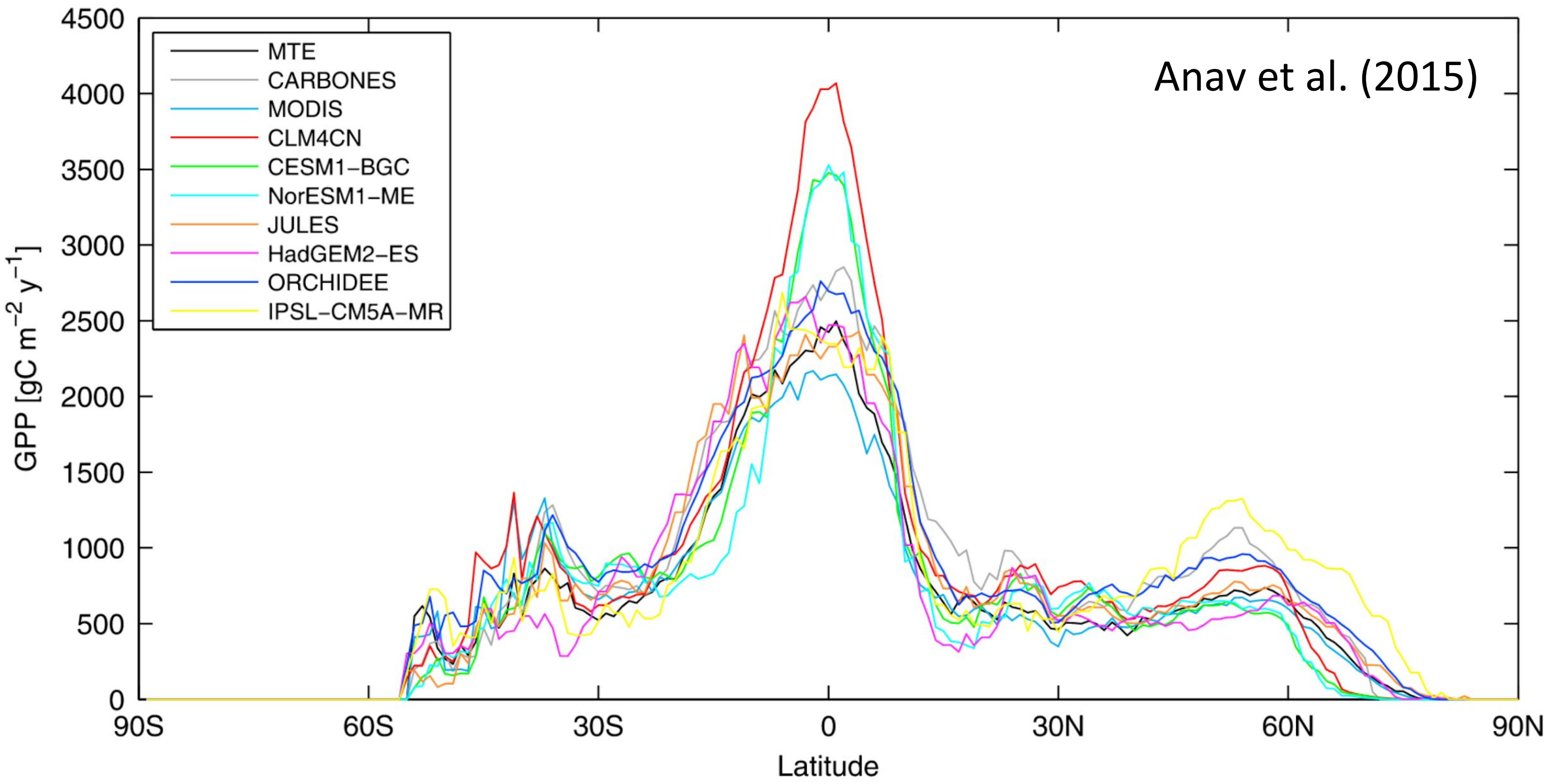

GPP and SIF

- Linear relationship at monthly timescale
- Slope can vary with ecosystem type and environmental conditions

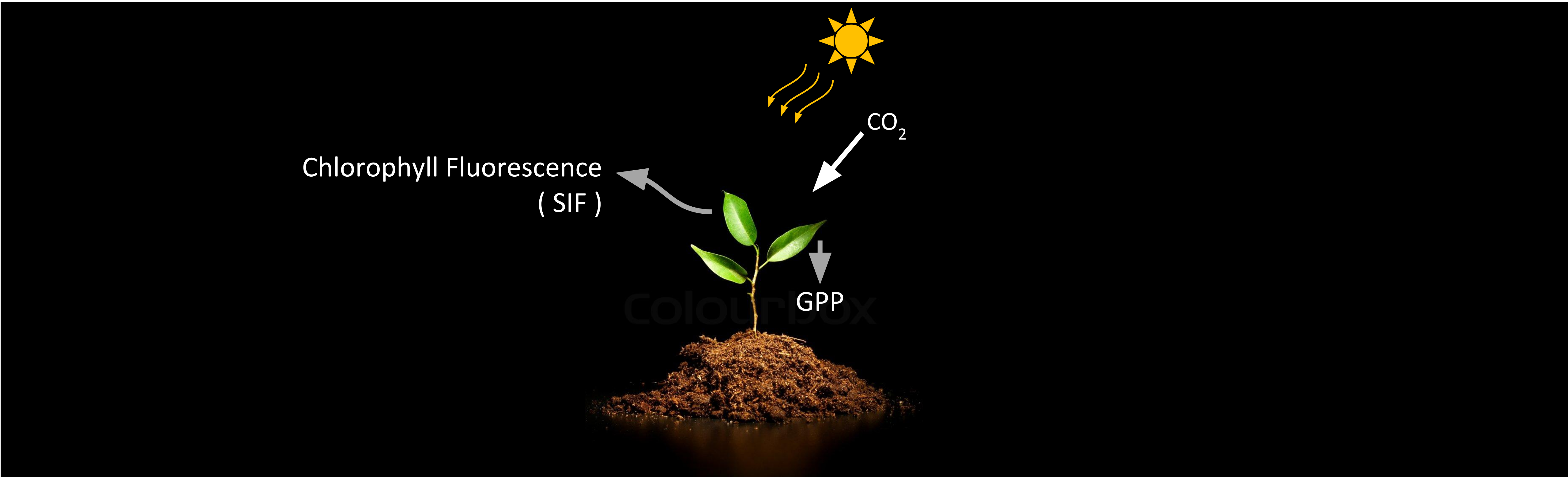

Using SIF to Constrain GPP

- Can use a simple linear scaling (e.g. Macbean et al. 2018):
  - This may omit some important non-linearities
  - Cause additional equifinality issues

- Can use a more complex model:
  - Better basis for prediction
  - Semi-empirical models e.g. Guan et al. (2015), Zhang et al. (2018)
  - More mechanistic models e.g. Koffi et al. (2015), Norton et al. (2018)

We use the SCOPE model embedded within the land surface model BETHY to simulate SIF and GPP globally.

- This provides a mechanistic relationship between SIF and GPP
- So, the relationship is described by processes, not linear scaling parameters

THE UNIVERSITY OF MELBOURNE

Our Data Assimilation Framework

- We use a variational data assimilation system:
  - Apply a quasi-Newton minimization algorithm (Tarantola, 2005)
  - It is iterative
  - The Jacobian (sensitivities) is re-calculated after each iteration to account for non-linearities (this has a large computational demand)

Minimizes a global cost function that describes the mismatch between the model and observations weighted by their uncertainties.

BETHY-SCOPE

Carbon Cycle Model

Photosynthesis
Chlorophyll Fluorescence
Plant Growth
Plant & Soil Respiration

+

OCO-2 Satellite [2015]

SIF Observations

→

Data Assimilation Algorithm

Optimize Model Parameters

Estimate GPP

The Model

The BETHY-SCOPE Model

- Simulates SIF and GPP globally at 2° x 2°
- 13 PFTs (can have 3 PFTs per pixel)
- BETHY provides the infrastructure to simulate SCOPE globally.
  - It can also simulate prognostic LAI and provide it to SCOPE.
- SCOPE simulates SIF and GPP
  - It is 1D (i.e. no horizontal variation in canopy structure)
  - Not a full SVAT model, but it simulates SIF mechanistically
- Process parameters can be PFT-specific (e.g. V_{cmax}), PFT-grouped (e.g. LIDF) or global (e.g. Michaelis-Menten kinetic constants).
- Leaf Area Index (LAI) is prescribed
  - We use “MODIS Improved” dataset (Yuan et al., 2011)

For more information see: Rayner et al. (2005); Knorr et al. (2010); Koffi et al. (2015); Norton et al. (2018)

The SIF Observations

OCO-2 SIF

- Gridded to 2° x 2° and monthly scales
- We use:
  - 2015 for optimization/calibration
  - Sep-Dec 2014 for validation
- Calculated uncertainties:
  - We don't use the standard error
  - Calculated uncertainties are between standard error and average of single measurement precision error
- Data over water (IGBP) are omitted

Mean SIF for 2015

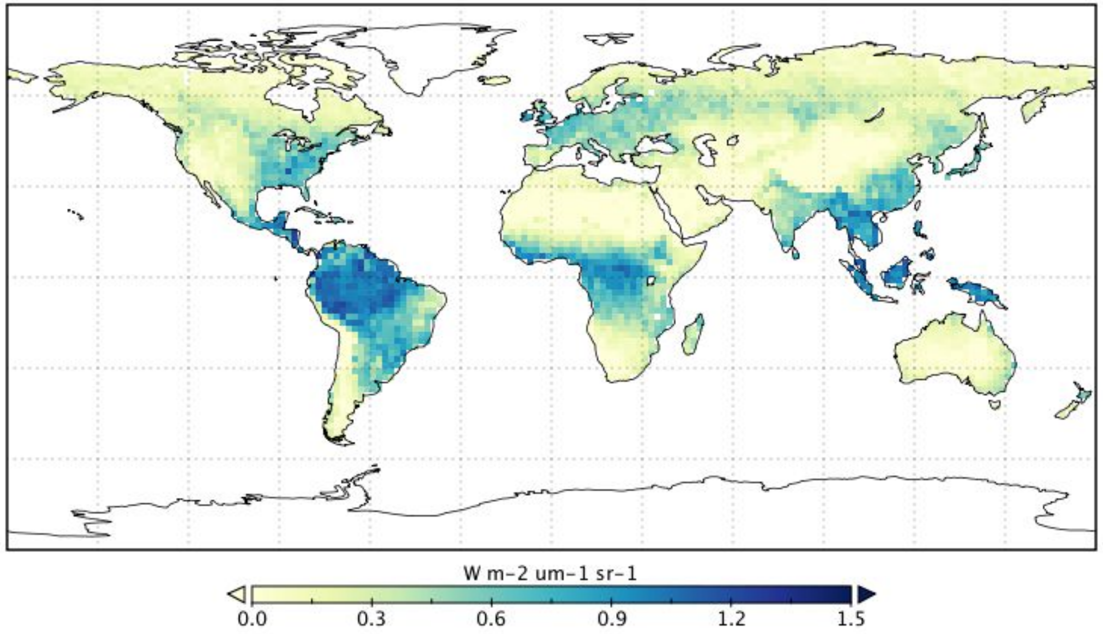

OCO-2 SIF Uncertainty for January 2015

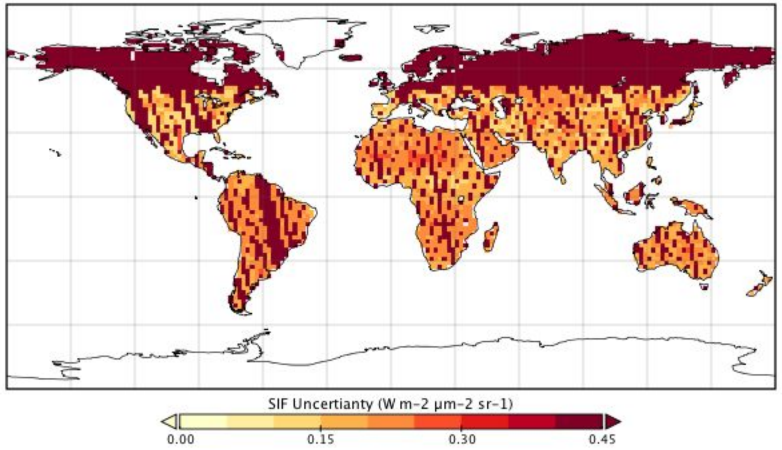

OCO-2 SIF Uncertainty for July 2015

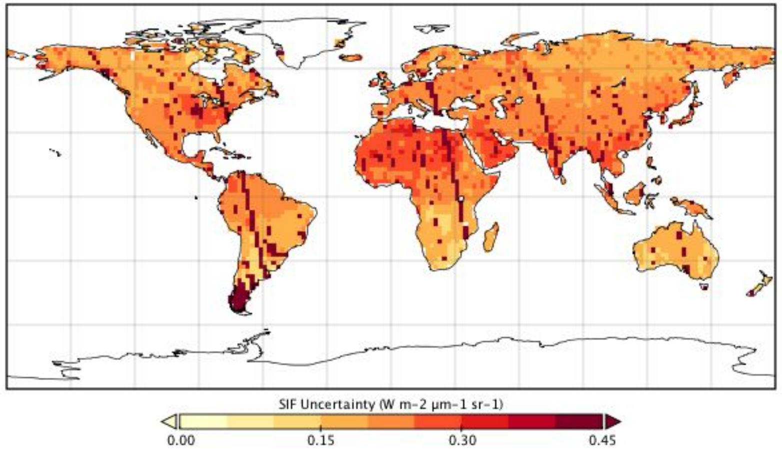

Model vs Observations: Prior

For calibration period (2015)

$$SIF\ Residual = Model - Observed$$

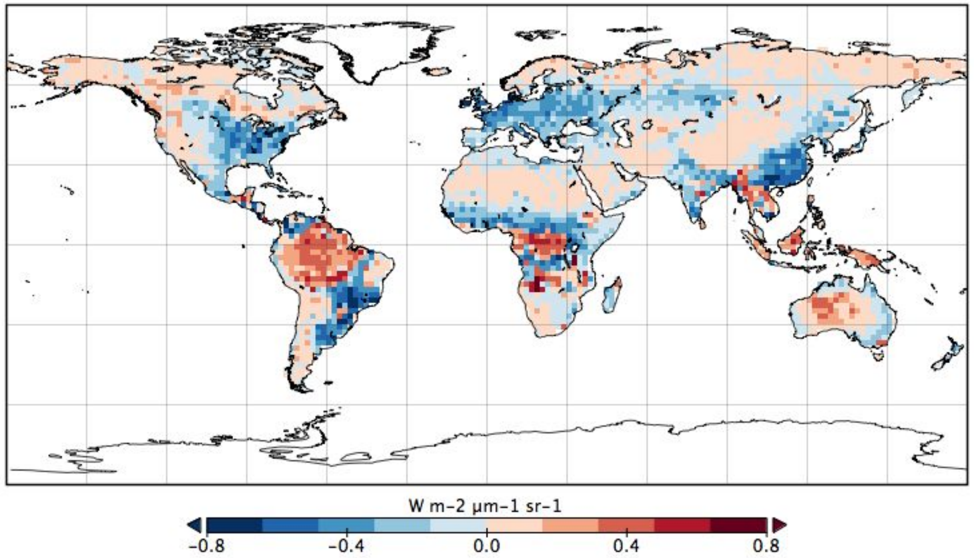

$$SIF\ Mismatch = \frac{Model - Observed}{Uncertainty}$$

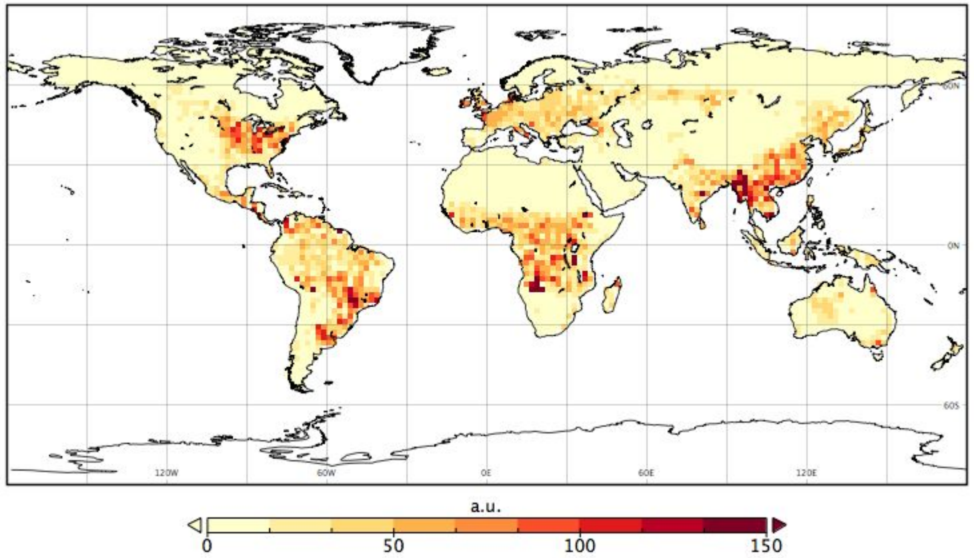

Model vs Observations: Posterior

For calibration period (2015)

$$SIF\ Residual = Model\ - Observed$$

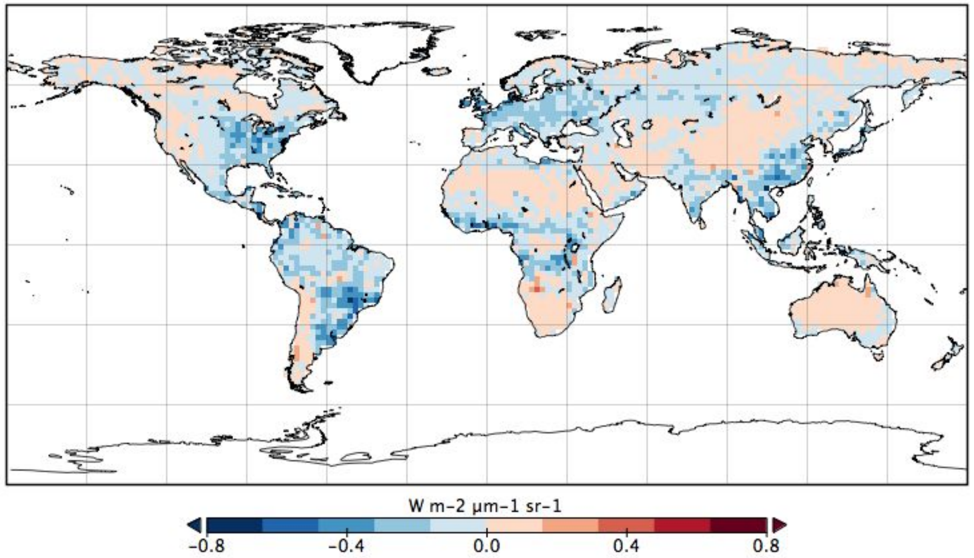

$$SIF\ Mismatch = \frac{Model\ - Observed}{Uncertainty}$$

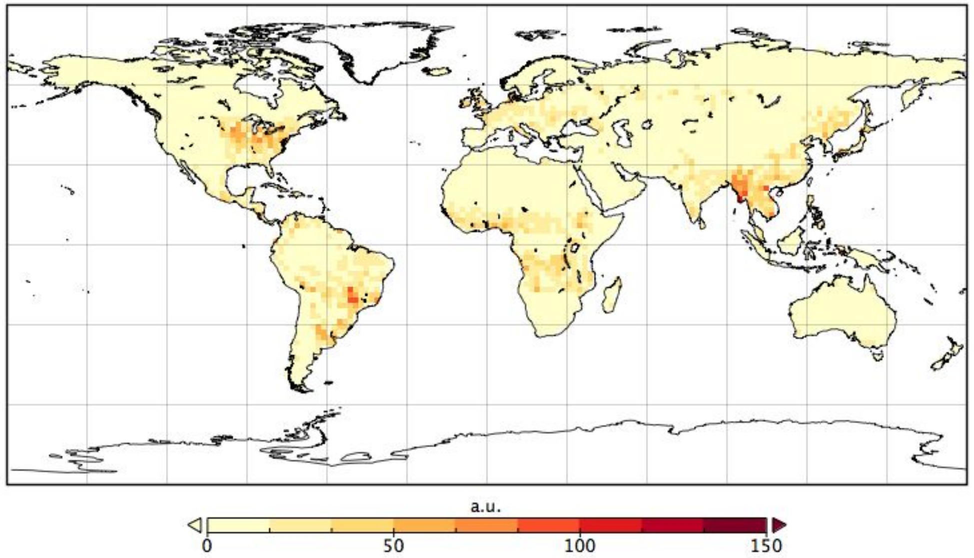

Model vs Observations

Prior
(2015)

Posterior
(2015)

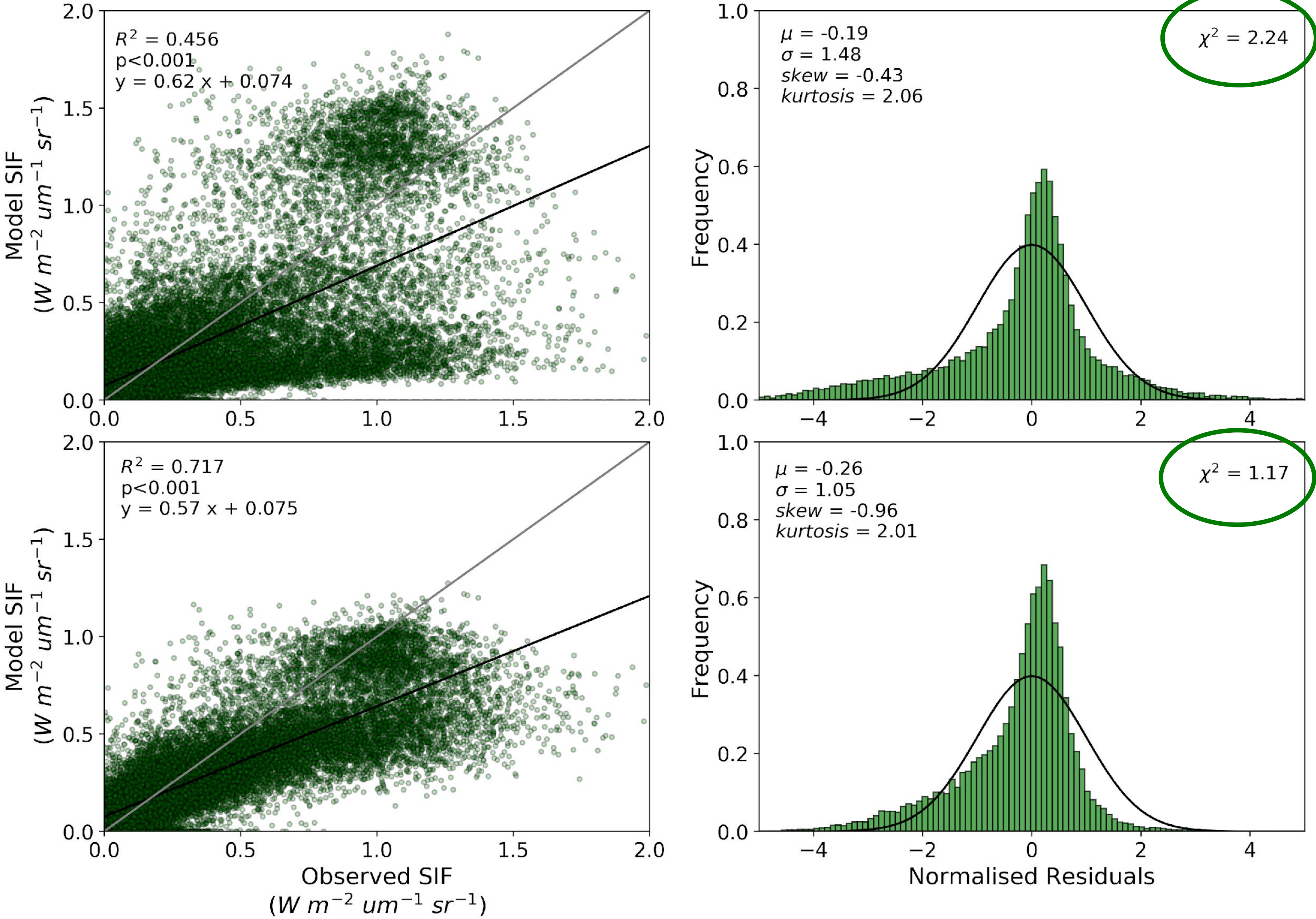

Model vs Observations: Validation

Prior
(Sep-Dec 2014)

Posterior
(Sep-Dec 2014)

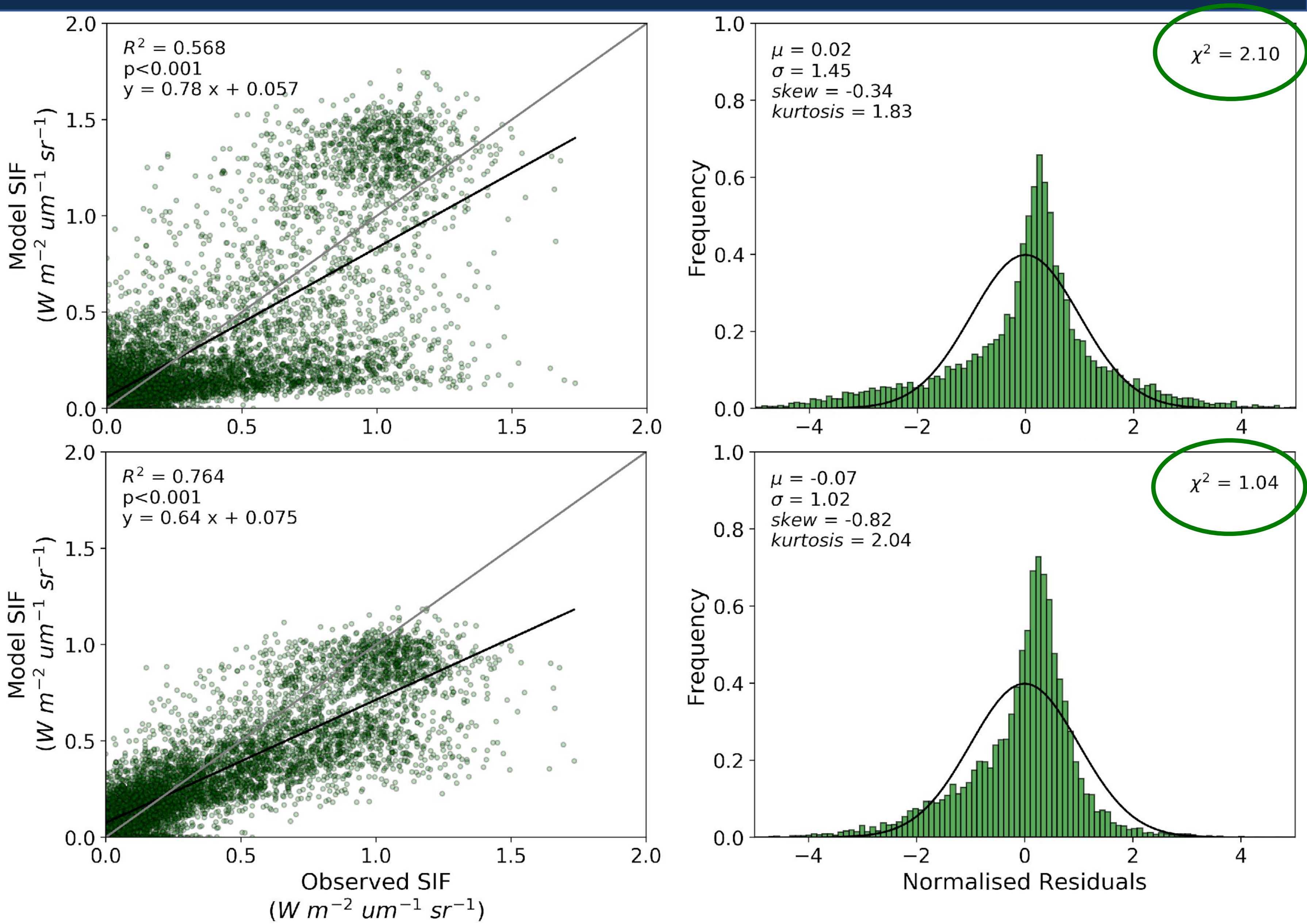

Optimization

- An optimal fit, given the uncertainties, will give:
$$\chi_r^2 = 1$$

Calibration period (2015):

Prior: $\chi_r^2 = 2.24$

Posterior: $\chi_r^2 = 1.18$

Validation period (Sep-Dec 2014):

Prior: $\chi_r^2 = 2.10$

Posterior: $\chi_r^2 = 1.04$

We are fitting the data well and not overfitting!

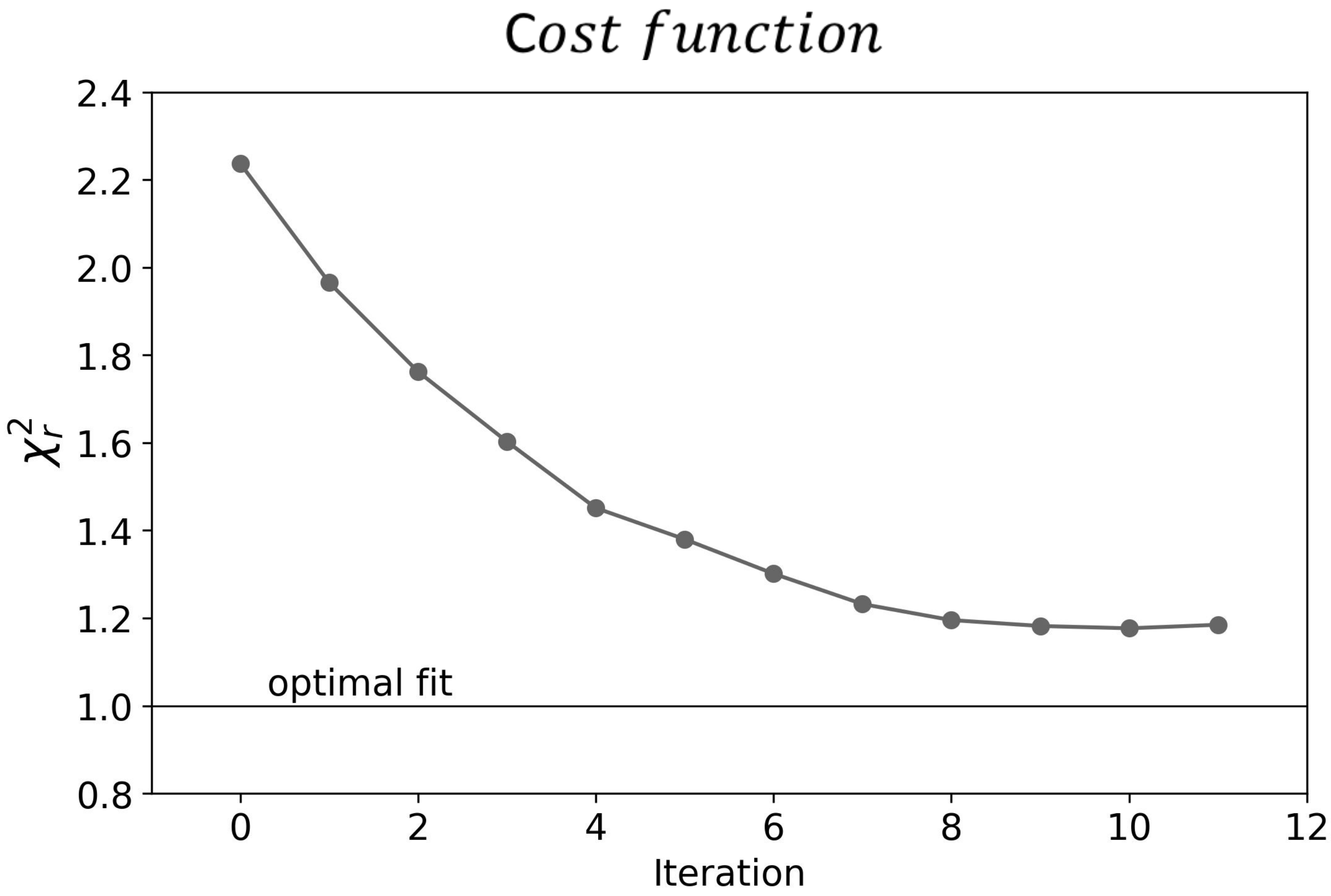

Optimized Parameters

42 parameters are exposed to the optimization: each is represented by a Gaussian PDF.

Following the assimilation of SIF:

- Chlorophyll content decreases (except C3 grass):
  - Posterior estimates range from 1-13 μg cm^{-2}
  - Strong reduction of uncertainty (typically around 90%)
- V_{cmax} generally increases:
  - Posterior estimates range from 11-125 μmol m^{-2} s^{-1}
  - Weak reduction of uncertainty (typically < 10%)
- Little change in other physiology parameters (e.g. K_C, K_O)
- Varied changes to canopy structure (e.g. LIDFa, LIDFb)

Remember that LAI is prescribed and therefore fixed.

SIF-Optimized GPP (2015)

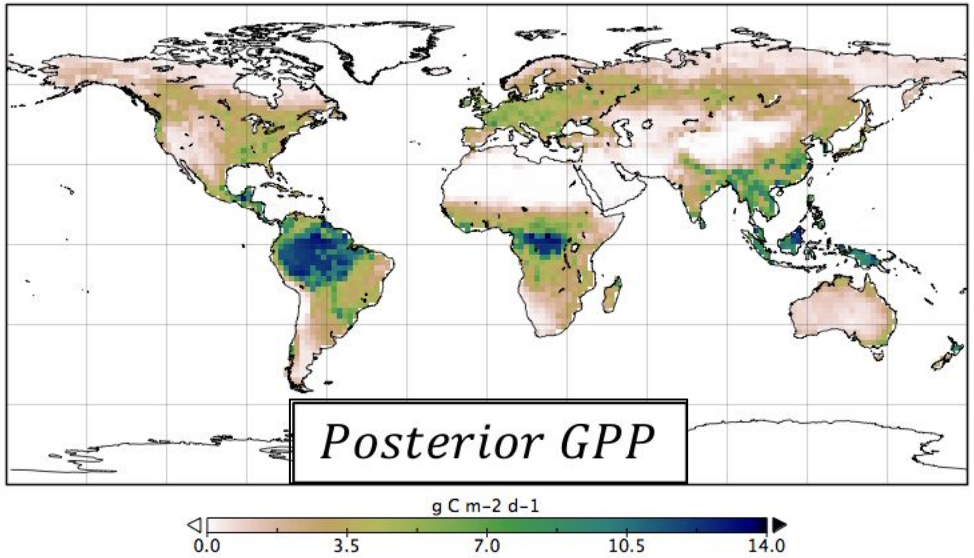

ΔGPP (%)

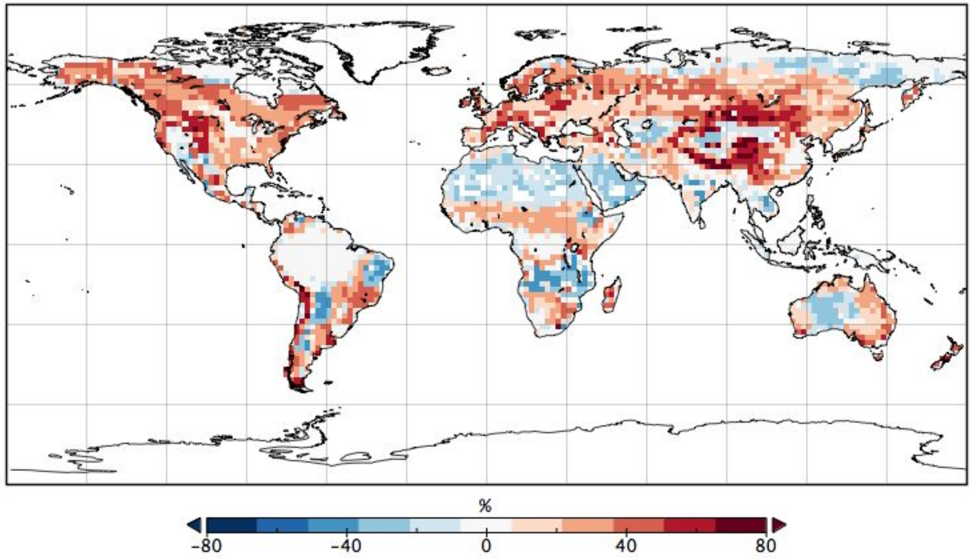

ΔGPP

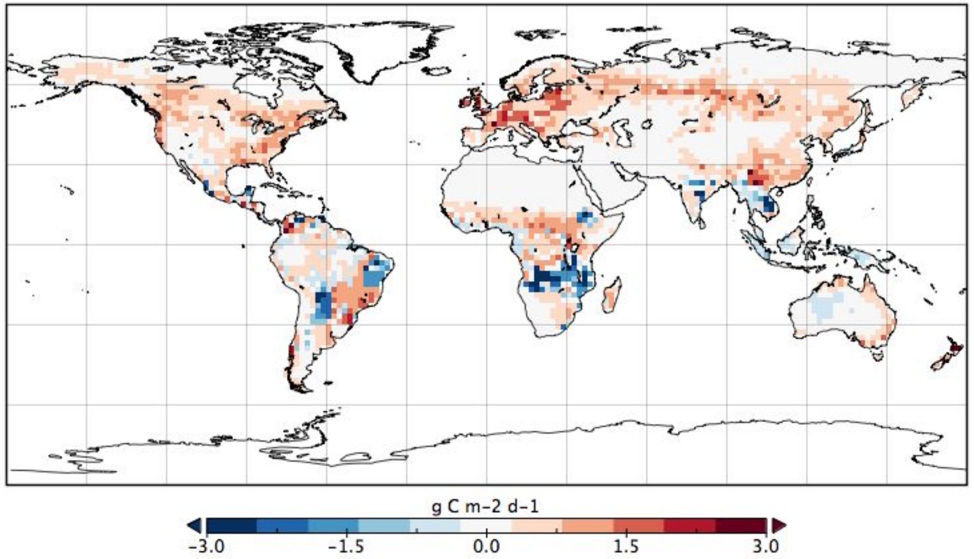

- Increase in extra-tropics.
- Decreases in dry tropics (forests + grasslands).
- Little change in wet tropical forests.

Overall increase in global annual GPP from
128 Pg C → 137 Pg C

SIF-Optimized GPP (2015)

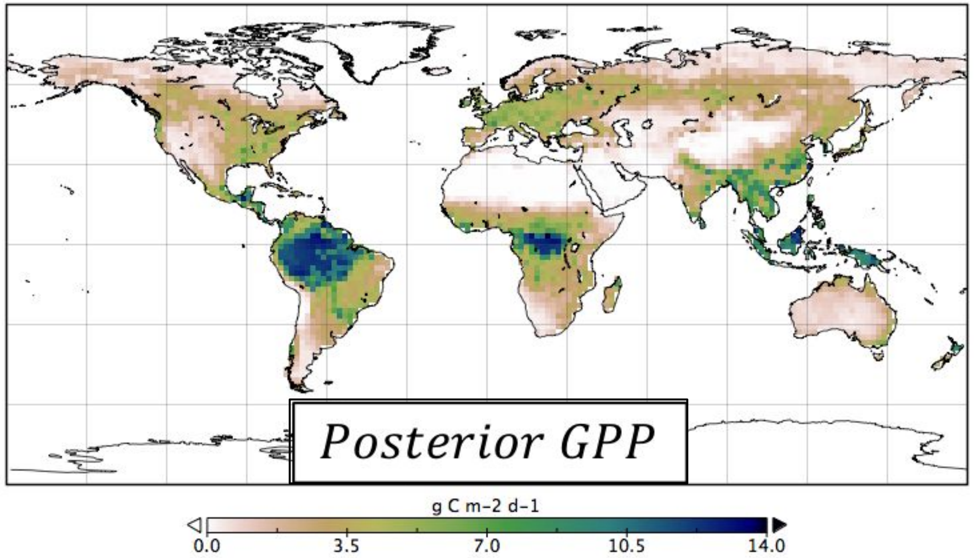

The uncertainty in GPP due to uncertain parameters is reduced by 65% by the SIF observations.

- Global annual GPP:

  Prior = 128 ± 17 Pg C

  Posterior = 137 ± 6 Pg C

SIF-Optimized GPP (2015)

Overall the spatial patterns look reasonable.

Compared to other GPP estimates, our SIF-optimized GPP is:

- Relatively high in the tropics and the temperate north
- Higher than FLUXCOM GPP almost everywhere (except north of 65° N)

Global GPP:

Prior	= 128 Pg C
Posterior. (SIF)	= 137 Pg C
TRENDY	= 142 Pg C
FLUXCOM	= 103 Pg C

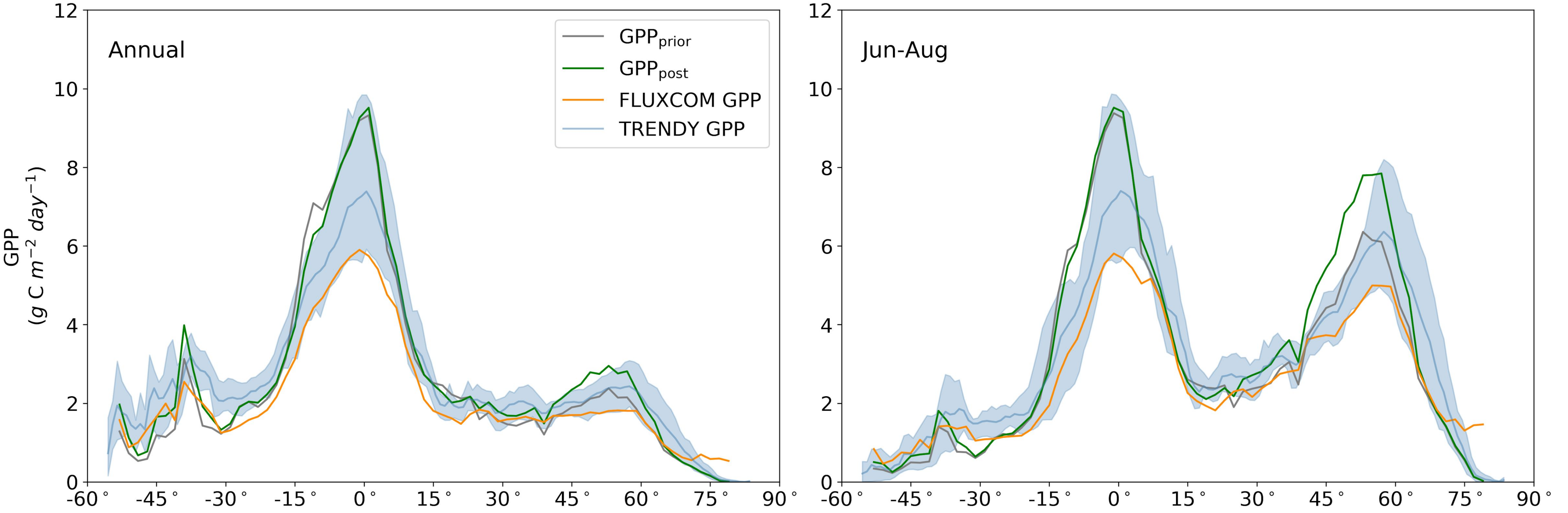

THE UNIVERSITY OF MELBOURNE

SIF-Optimized GPP (2015)

What causes the change in GPP following the SIF assimilation?

- APAR decreases globally
  - Due to decline in chlorophyll
- LUE increases globally
  - Due to decline in APAR
  - Due to increase in V_{cmax}

APAR
(% change)

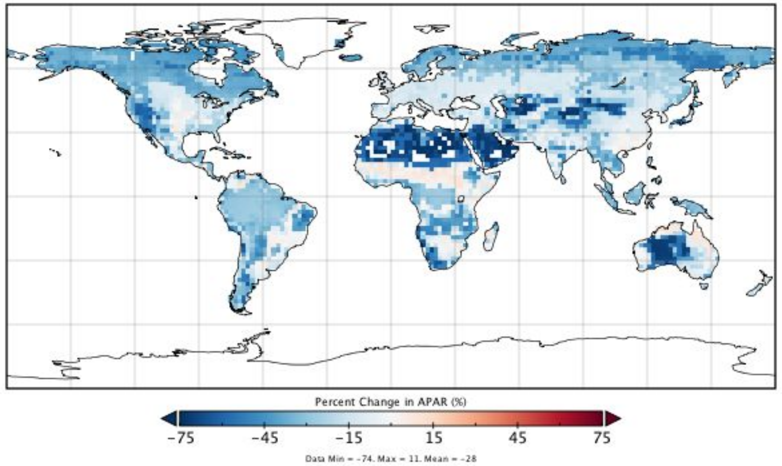

LUE
(% change)

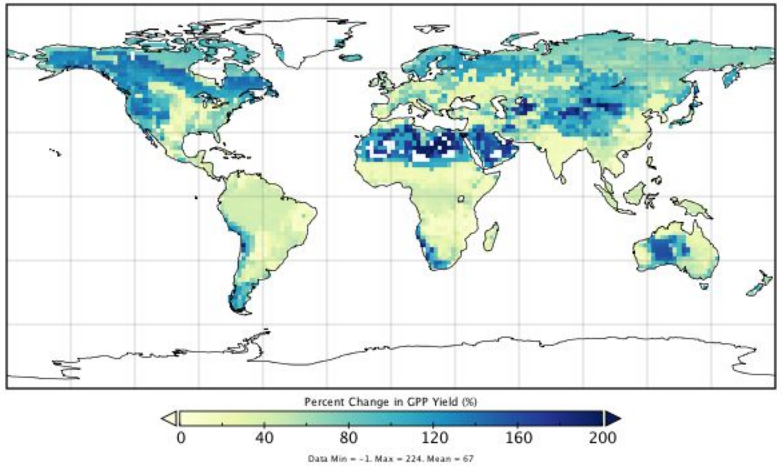

Remaining Challenges

- The model struggles to simultaneously fit low and high SIF values (> 1.0 W m-2).

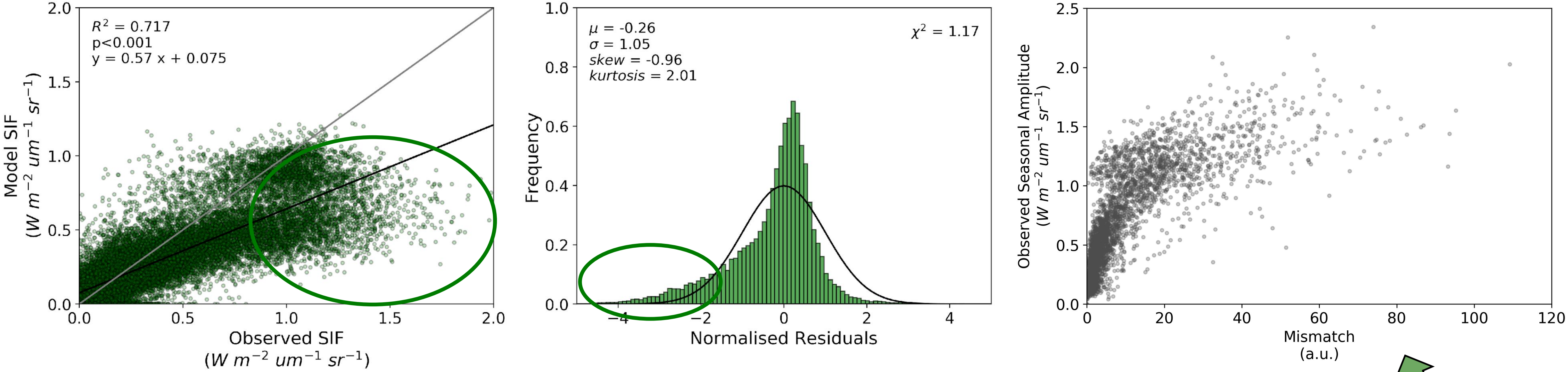

Ecosystems with a large seasonal cycle in OCO-2 SIF show the largest model-observed mismatch. Why?

- Parameters (e.g. chlorophyll, V_{cmax}, LIDF) probably vary seasonally, we keep them constant.
- Issues with prescribed LAI?
- Issues with spatial averaging differences between SIF, LAI, climate variables?

THE UNIVERSITY OF MELBOURNE

Remaining Challenges

- The model struggles to simultaneously fit low and high SIF values (> 1.0 W m-2).

→ Seasonal variation in parameters would help fit the data and be more realistic.

SIF GPP LAI

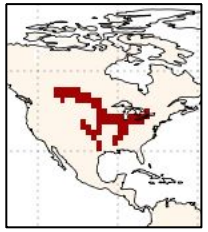

North America Croplands

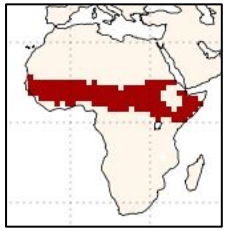

Northern Africa Savanna

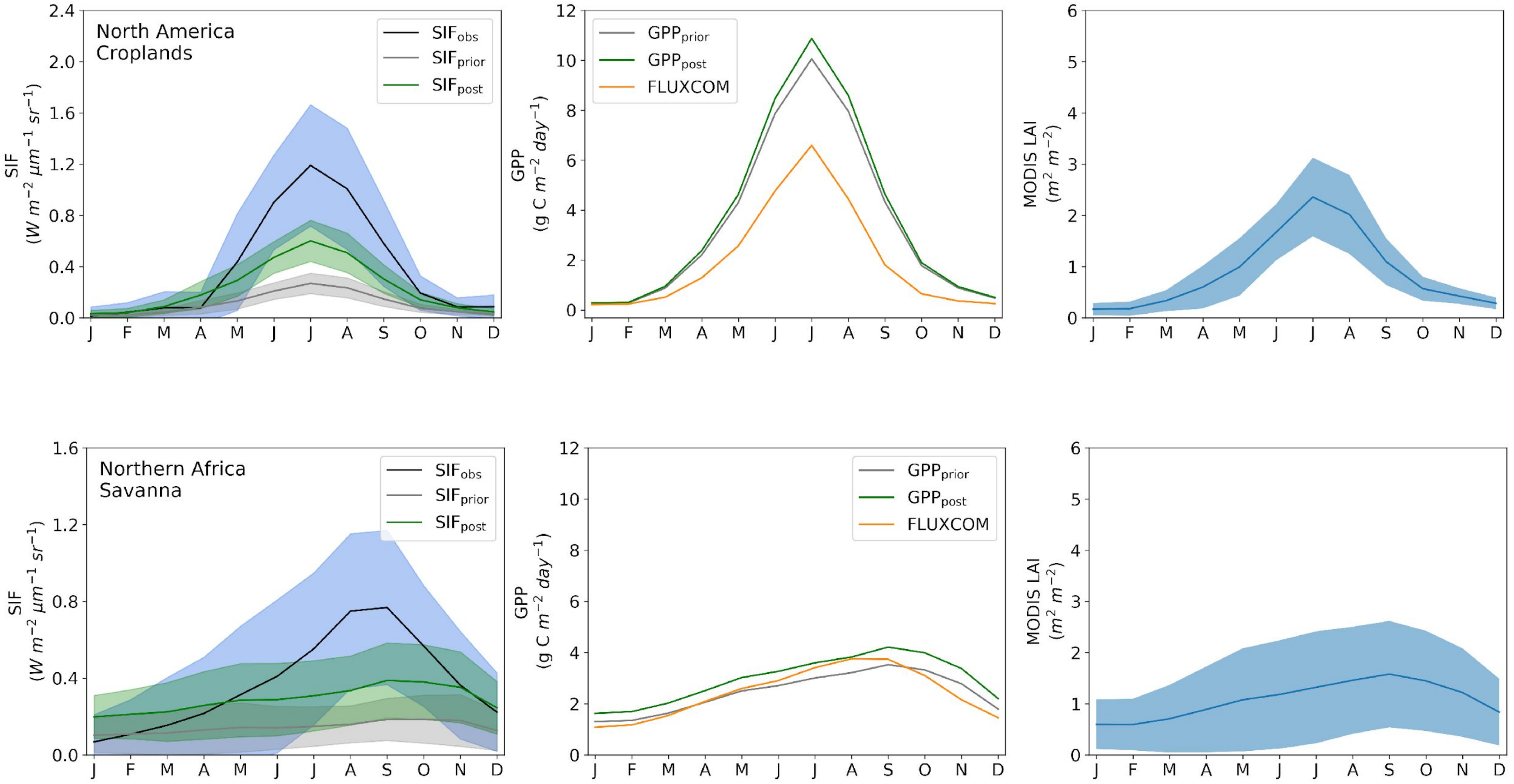

Remaining Challenges

- The model struggles to simultaneously fit low and high SIF values (> 1.0 W m-2).

⟶ Seasonal cycle in LAI is vastly different to SIF in some regions

⟶ Shown here: SIF peaks in July-August but LAI peaks in November (LAI retrieval issues?)

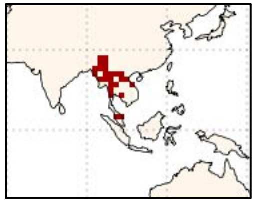

S.E. Asia Tropical Forest

SIF

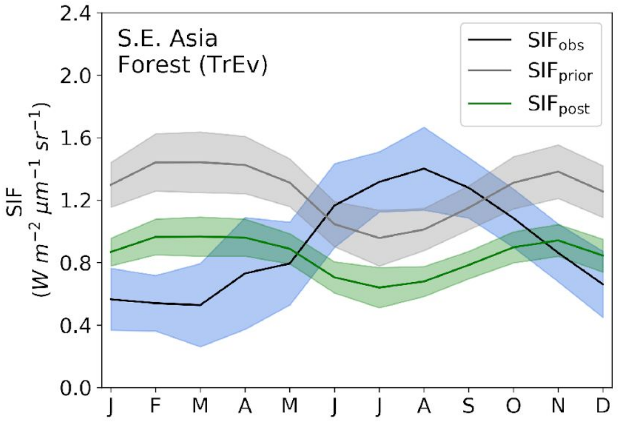

GPP

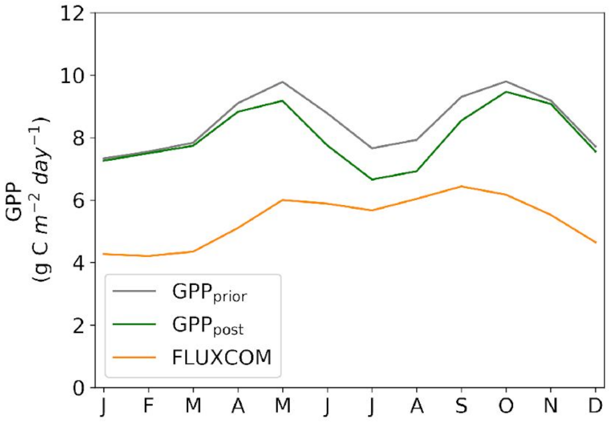

LAI

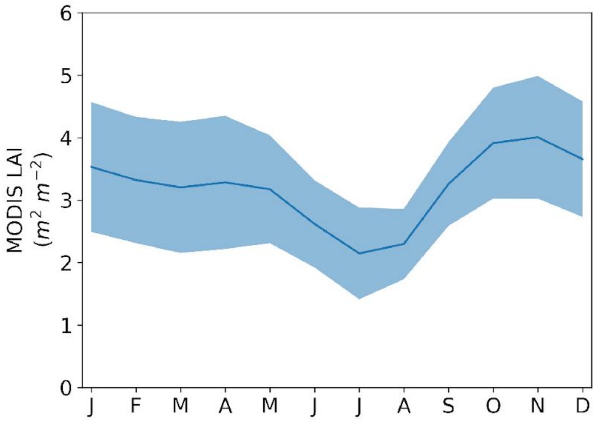

Remaining Challenges

- Validating parameters (e.g. chlorophyll, V_{cmax}) and derived variables (e.g. APAR, LUE).

→ Very challenging at this scale!

→ We could evaluate against site-based data: issues with representativity

→ We could evaluate chlorophyll against the MERIS Terrestrial Chlorophyll Index

→ We're open to suggestions!

Remaining Challenges

- Validating GPP

→ Also very challenging at this scale

→ Test: Does the SIF-optimized model improve our match with atmospheric CO_2 or COS?

→ Comparison with FLUXCOM GPP over North America and Europe (where density of flux towers is higher) suggest the general patterns are decent:

  - The correlation with FLUXCOM GPP improves following the SIF assimilation.
  - However, the SIF-optimized GPP magnitude is larger.
  - We wouldn't do this for the tropics!

North America

R^2 (prior) = 0.80

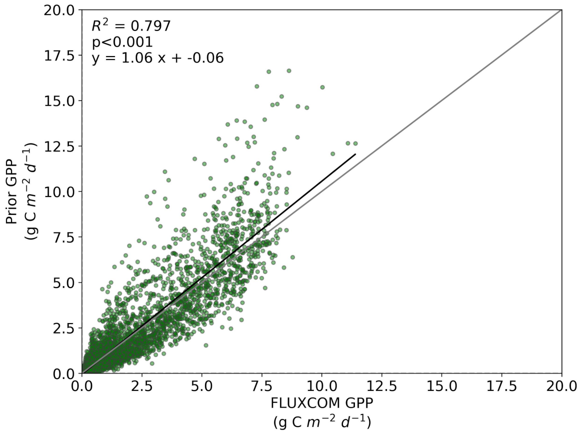

R^2 (post.) = 0.86

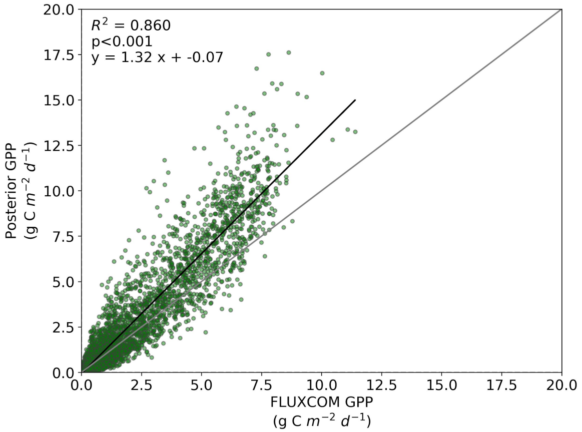

Europe

R^2 (prior) = 0.77

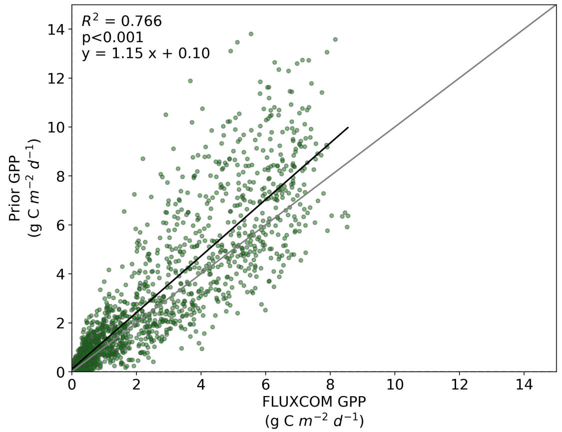

R^2 (post.) = 0.83

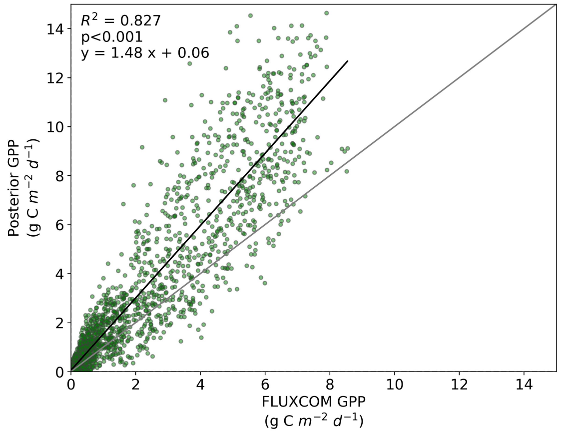

Next Steps

- Interannual variability: can the optimized model capture IAV in SIF?
- Conduct a similar optimization at sites.
- Use complementary observations (e.g. FAPAR, NIRv): use these to constrain chlorophyll and/or LAI first.

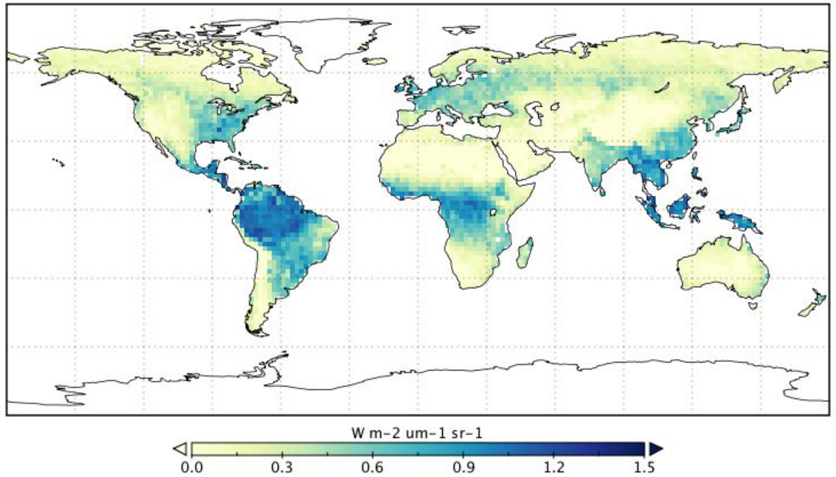

OCO-2 SIF

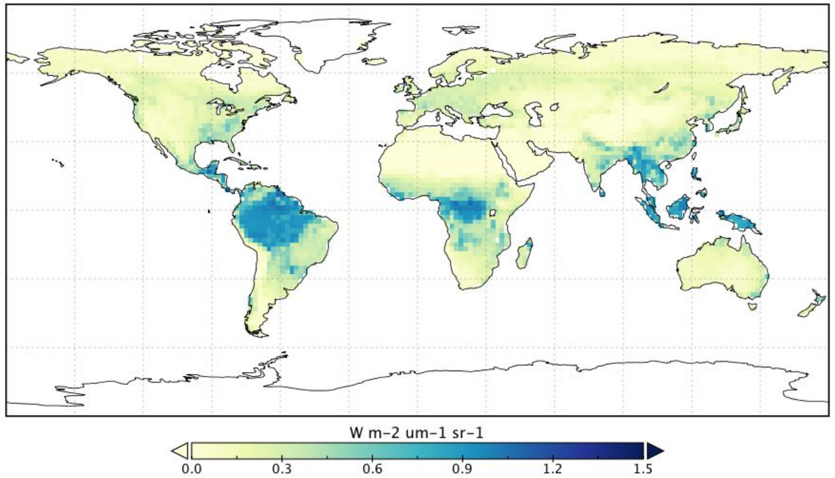

BETHY-SCOPE SIF (post.)

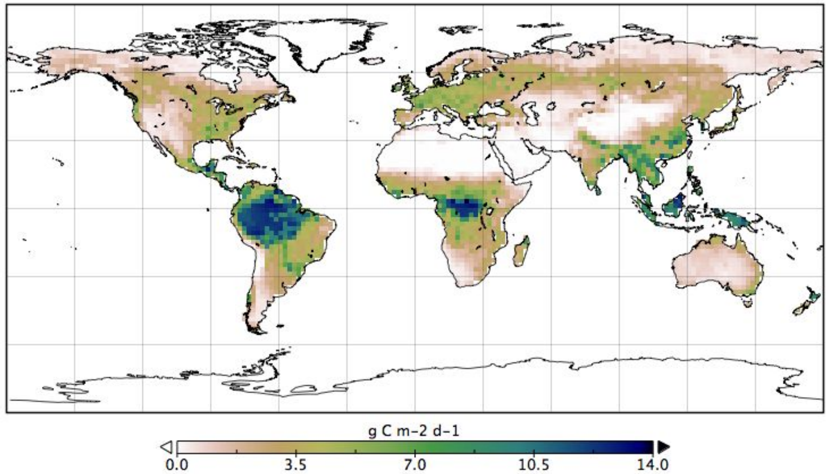

BETHY-SCOPE GPP (post.)

Thank you!

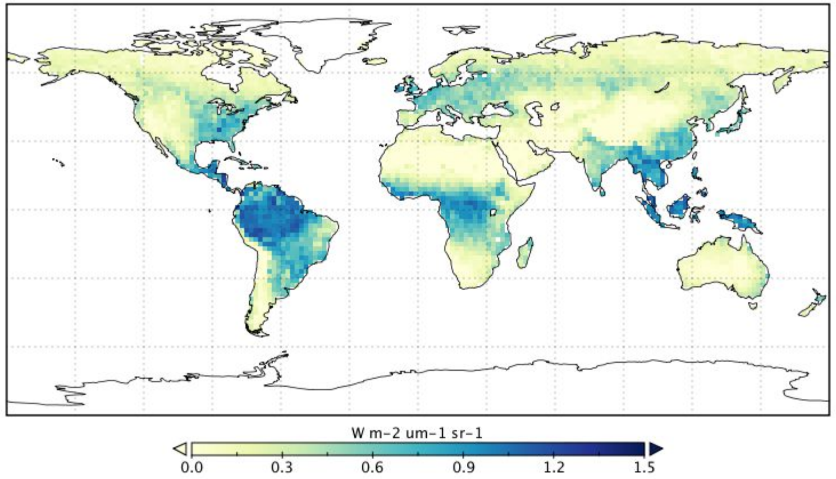

OCO-2 SIF

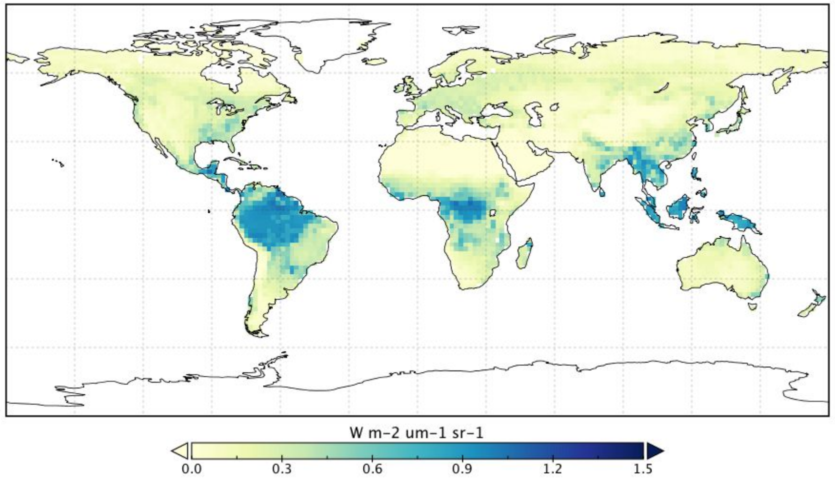

BETHY-SCOPE SIF (post.)

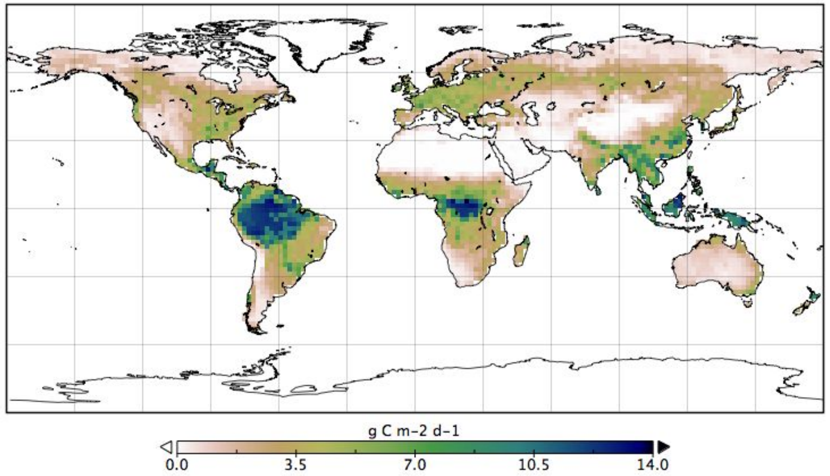

BETHY-SCOPE GPP (post.)

References

Anav, A., Friedlingstein, P., Beer, C., Ciais, P., Harper, A., Jones, C., Murray-Tortarolo, G., Papale, D., Parazoo, N. C., Peylin, P., Piao, S., Sitch, S., Viovy, N., Wiltshire, A., and Zhao, M.: Spatiotemporal patterns of terrestrial gross primary production: A review, Reviews of Geophysics, 53, 785–818, https://doi.org/10.1002/2015RG000483, 2015.

Guan, K., Berry, J., Zhang, Y., Joiner, J., Guanter, L., Badgley, G., Lobell, D.: Improving the monitoring of crop productivity using spaceborne solar-induced fluorescence, Global Change Biology, 22, 716-726, doi: 10.1111/gcb.13136, 2015

Knorr, W., Kaminski, T., Scholze, M., Gobron, N., Pinty, B., Giering, R., and Mathieu, P.-P.: Carbon cycle data assimilation with a generic phenology model, Journal of Geophysical Research, 115, G04 017, https://doi.org/10.1029/2009JG001119, 2010.

Koffi, E. N., Rayner, P. J., Norton, A. J., Frankenberg, C., and Scholze, M.: Investigating the usefulness of satellite-derived fluorescence data in inferring gross primary productivity within the carbon cycle data assimilation system, Biogeosciences, 12, 4067–4084, https://doi.org/10.5194/bg-12-4067-2015, 2015

MacBean, N., Maignan, F., Bacour, C., Lewis, P., Peylin, P., Guanter, L., Köhler, P., Gómez-Dans, J., and Disney, M.: Strong constraint on modelled global carbon uptake using solar-induced chlorophyll fluorescence data, Scientific Reports, 8, 1–12, https://doi.org/10.1038/s41598-018-20024-w, 2018

Norton, A. J., Rayner, P. J., Koffi, E. N., and Scholze, M.: Assimilating solar-induced chlorophyll fluorescence into the terrestrial biosphere model BETHY-SCOPE v1.0: model description and information content, Geoscientific Model Development, 11, 1517–1536, https://doi.org/10.5194/gmd-11-1517-2018, https://www.geosci-model-dev-discuss.net/gmd-2017-34/https://www.geosci-model-dev.net/11/1517/2018/, 2018.

Rayner, P., Scholze, M., Knorr, W., and Kaminski, T.: Two decades of terrestrial carbon fluxes from a carbon cycle data assimilation system (CCDAS), Biogeochemical Cycles, 19, GB2026, https://doi.org/10.1029/2004GB002254, 2005.

Tarantola, A.: Inverse Problem Theory and Methods for Model Parameter Estimation, SIAM, Philadelphia, 2005

Yuan, H., Dai, Y., Xiao, Z., Ji, D., and Shangguan, W.: Reprocessing the MODIS Leaf Area Index products for land surface and climate modelling, Remote Sensing of Environment, 115, 1171–1187, https://doi.org/10.1016/j.rse.2011.01.001, http://dx.doi.org/10.1016/j.rse.2011.01.001, 2011.

Zhang, Y., Guanter, L., Joiner, J., Song, L., Guan, K.: Spatially-explicit monitoring of crop photosynthetic capacity through the use of space-based chlorophyll fluorescence data, Remote Sensing of Environment, 210, 362-374, https://doi.org/10.1016/j.rse.2018.03.031